Title	A screen-printed CPW-fed circularly polarized antenna using a sustainable cork substrate
Authors	Kumar, Sanjeev;Moloudian, Gholamhosein;Gawade, Dinesh R.;Iacopino, Daniela;O'Flynn, Brendan;Buckley, John L.
Publication date	2025
Original Citation	Kumar, S, Moloudian, G, Gawade, D R, Iacopino, D, O'Flynn, B & Buckley, J L 2025, A screen-printed CPW-fed circularly polarized antenna using a sustainable cork substrate. in 2025 19th European Conference on Antennas and Propagation (EuCAP). 19th European Conference on Antennas and Propagation, EuCAP 2025, Stockholm, Sweden, 30/03/25. https://doi.org/10.23919/EuCAP63536.2025.10999358
Type of publication	Conference item
Link to publisher's version	https://www.scopus.com/pages/publications/105007498279 - 10.23919/EuCAP63536.2025.10999358
Rights	© 2025, IEEE. Personal use of this material is permitted. Permission from IEEE must be obtained for all other uses, in any current or future media, including reprinting/republishing this material for advertising or promotional purposes, creating new collective works, for resale or redistribution to servers or lists, or reuse of any copyrighted component of this work in other works.
Download date	2026-09-18 23:10:49
Item downloaded from	https://hdl.handle.net/10468/18503

A Screen-Printed CPW-Fed Circularly Polarized Antenna Using a Sustainable Cork Substrate

Sanjeev Kumar, Gholamhosein Moloudian, Dinesh R Gawade, Daniela Iacopino, Brendan O'Flynn, and John L. Buckley
Tyndall National Institute, University College Cork, Dyke Parade, T12R5CP, Cork, Ireland
Email:sanjeev.kumar@tyndall.ie

***Abstract*—This paper presents a novel, coplanar waveguide (CPW)-fed circularly polarized (CP) monopole antenna. The antenna is fabricated using screen-printing techniques, with silver nanoparticles as the conductive material and cork used as a sustainable substrate. Circular polarization is achieved by introducing a radiating element orthogonal to the main radiating monopole element. The measurements of the fabricated antenna show a -10 dB impedance bandwidth of 183 MHz, corresponding to a fractional bandwidth (FBW) of 7.6% at 2.4 GHz. Furthermore, at 2.4 GHz, the antenna demonstrates a measured peak realized gain of -1.8 dBi and a radiation efficiency of 58%. A 3-dB axial-ratio fractional bandwidth for right-hand circular polarization (RHCP) operation at 2.4 GHz is 5.3%. The proposed antenna is well-suited for use in various 2.4 GHz wireless local area network (WLAN) technologies, such as Bluetooth and Wi-Fi, and can be integrated into items such as next-generation smart floors using sustainable materials.**

***Index Terms*—Screen-printed, sustainable cork substrate, circular polarization (CP), axial ratio (AR), monopole antenna.**

I. Introduction

In recent years, there has been a growing interest in utilizing sustainable, biodegradable natural materials combined with non-conventional manufacturing processes to develop eco-friendly antennas and radio frequency (RF) components for next-generation wireless solutions [1], [2]. Conventional antennas are typically fabricated using printed circuit board (PCB) technology with rigid substrates, such as FR4 and Rogers materials [3]. While these substrates provide excellent mechanical and electrical properties, their non-biodegradable nature raises significant environmental concerns. To address these challenges, recent research has increasingly focused on using sustainable, eco-friendly and recyclable materials as substrates [2], [4]. Cork, a natural and biodegradable material, has garnered significant attention in the design of antennas and RF components due to its potential to reduce the environmental impact of electronic devices [1], [2]. Beyond its sustainability, cork offers several advantageous properties, including cost-effectiveness, a lightweight structure, flexibility, thermal insulation and a low dielectric constant, making it a suitable candidate for developing RF antennas [1], [2], [5].

However, the current literature indicates that there has been limited research on the development of RF antennas using a cork substrate [1], [2], [6]–[9]. In [1], a 915 MHz ultra-high frequency (UHF) meandered dipole antenna, designed for RFID applications in the identification of wine bottles and barrels is reported. The antenna's conductive strips are fabricated by milling adhesive copper tape, which is then affixed to a cork substrate shaped like a wine bottle stopper. In [9], an 866 MHz UHF 3D meandered dipole antenna, designed to fit within a cork-based barrel stopper structure for an RFID-enabled temperature sensor, is presented. Similar to the antenna described in [1], this antenna [9] is also fabricated by milling the radiating structure onto copper tape and attaching it to a cork substrate. In [6]–[8], cork material has been used to develop substrate-integrated waveguide (SIW) cavity-backed slot antennas for the 5 GHz Wi-Fi band [6], [7] and ultra-wideband (UWB) applications [8], with the potential to be directly integrated into wooden floors or walls. The conductive parts of these SIW antennas are patterned using copper-plated taffeta electro-textile, which is adhered to the cork substrate with a thermally activated adhesive. In [2], a dual-band (868 MHz and 2.45 GHz) microstrip patch antenna, designed for integration into smart floors is developed using a biodegradable cork substrate. Similar to the antennas in [6]–[8], the radiating patches and ground plane of the antenna in [2] are patterned on taffeta electro-textile and laminated onto the cork substrate using thermally activated adhesive.

As described above, intricate fabrication methods have been employed for cork-based antennas reported in the existing literature. The reported fabrication process involves first producing the conductive parts of the antenna, either by milling copper tape [1], [9] or using taffeta electro-textile [2], [6]–[8], which are then attached to a cork substrate. Furthermore, circularly polarized (CP) antennas offer several benefits, including greater flexibility in antenna orientation, reduced polarization mismatch, and suppression of multipath interference [10]. However, none of the existing cork-based antennas are designed to achieve circularly polarized radiation characteristics.

This paper presents the design and development of a coplanar waveguide-fed CP antenna, which is fabricated on a cork substrate using a screen-printing technique with silver nanoparticles [11], [12]. The choice of screen printing is driven by its suitability for low-cost, scalable manufacturing and its compatibility with a diverse range of substrates, including flexible and porous materials such as cork [3], [12].

The remainder of the paper is organized as follows: Section II describes the design aspects of the proposed antenna. Section III presents the simulation results, including the antenna's

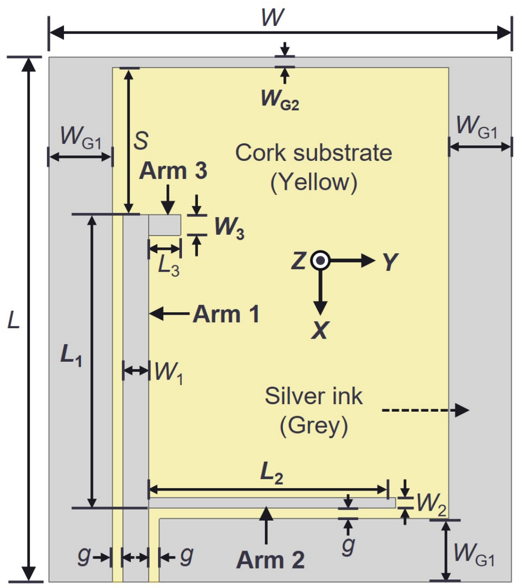

Fig. 1. Configuration of the proposed antenna (L = 50, W = 44, L_1 = 28, L_2 = 23.5, L_3 = 3, W_1 = 2.5, W_2 = 1, W_3 = 2, W_{G1} = 6, W_{G2} = 1, g = 1, S = 14; (Unit: mm).

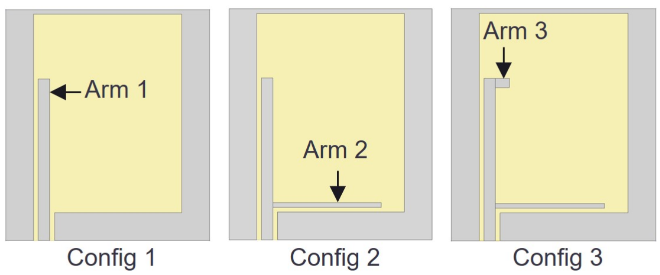

Fig. 2. Antenna design evolution.

operating principles, parametric analysis and surface current distribution. The antenna's fabrication method is detailed in Section IV. Section V discusses the measured results, and finally, Section VI summarizes the main conclusions of this work.

II. Antenna Design

The configuration on the proposed CPW-fed CP monopole antenna is shown in Fig. 1. The antenna is realized using a cork material as a substrate with a measured relative permittivity ϵ_r = 1.39 and loss tangent $tan\delta$ = 0.038 at 2.4 GHz. The dielectric properties of the cork material were derived using a dielectric assessment kit (DAK3.5-TL) from Speag [13]. For the conductive part of the antenna, commercially available screen-printable WIK21285-89A silver nanoparticle ink from Henkel was used [14]. The conductive layer was modeled as a 10 μm thick metal with a conductivity of 3.94×10^6 S/m at 2.4 GHz. The total size of the antenna is $50 \times 44 \times 1.6$ mm which corresponds to $0.47\lambda_g \times 0.41\lambda_g \times 0.015\lambda_g$, where λ_g = 106 mm is the guided wavelength in cork substrate at 2.4 GHz. The antenna is fed by 50-Ω coplanar waveguide (CPW) where

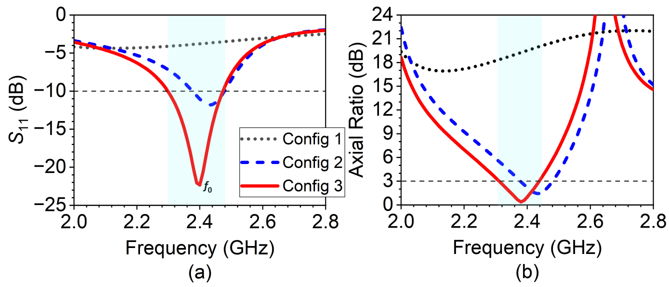

Fig. 3. Simulated S_{11} and axial ratio (AR) responses for the three antenna design evolution configurations shown in Fig. 2.

width of signal line is 2.5 mm and the gap between the signal line and the ground plane is 1 mm. The antenna configuration consists of two monopole radiating elements, denoted as Arm 1 ($L_1 = 0.26\lambda_g$) and Arm 2 ($L_2 = 0.22\lambda_g$). The rationale and design methodology for the proposed antenna structure are described in the following section.

III. Antenna Simulations

This section presents the simulated results of the proposed antenna. The antenna was designed using Ansys full-wave high- frequency structure simulator (HFSS) [15].

A. Antenna Operating Principle

To understand the operating principle, the design evolution of the antenna (Config 1 – Config 3) is demonstrated in Fig. 2. The corresponding simulated S_{11} and axial ratio (AR) responses for each design configuration are depicted in Fig. 3(a) and (b), respectively. The antenna design began with a CPW-fed single-element (Arm-1) monopole structure, denoted as Config 1. This Config 1 antenna exhibited poor impedance matching to 50-Ω and has linear polarization with an AR>18 dB at 2.4 GHz. It is known that CP characteristics can be achieved by exciting two orthogonal modes with equal amplitude and 90° phase difference [10]. Therefore, to achieve circular polarization, a horizontal element (Arm-2) was introduced, resulting in the antenna topology Config 2. The inclusion of Arm-2 excites the required phase perturbation to produce CP characteristics with AR<3 dB at 2.4 GHz. It can be seen form Fig. 3(a) and (b) that the inclusion of Arm-2 resulted in CP radiation, but with poor impedance matching to 50-Ω. Therefore, in the final stage, Arm-3 was incorporated to achieve the desired impedance matching while maintaining the CP response, resulting in the Config 3 topology (proposed antenna configuration). As shown in Fig. 3(b), the proposed antenna achieves a 3 dB AR bandwidth of 127 MHz, corresponding to an AR fractional bandwidth of 5.3% at 2.4 GHz.

B. Parametric Analysis

A parametric analysis was conducted to evaluate the effects of various antenna parameters (L_1, L_2, W_3, and W_{G2}) on the S_{11} and axial ratio (AR) responses of the antenna. When one parameter is varied, the others are kept constant. The effects of

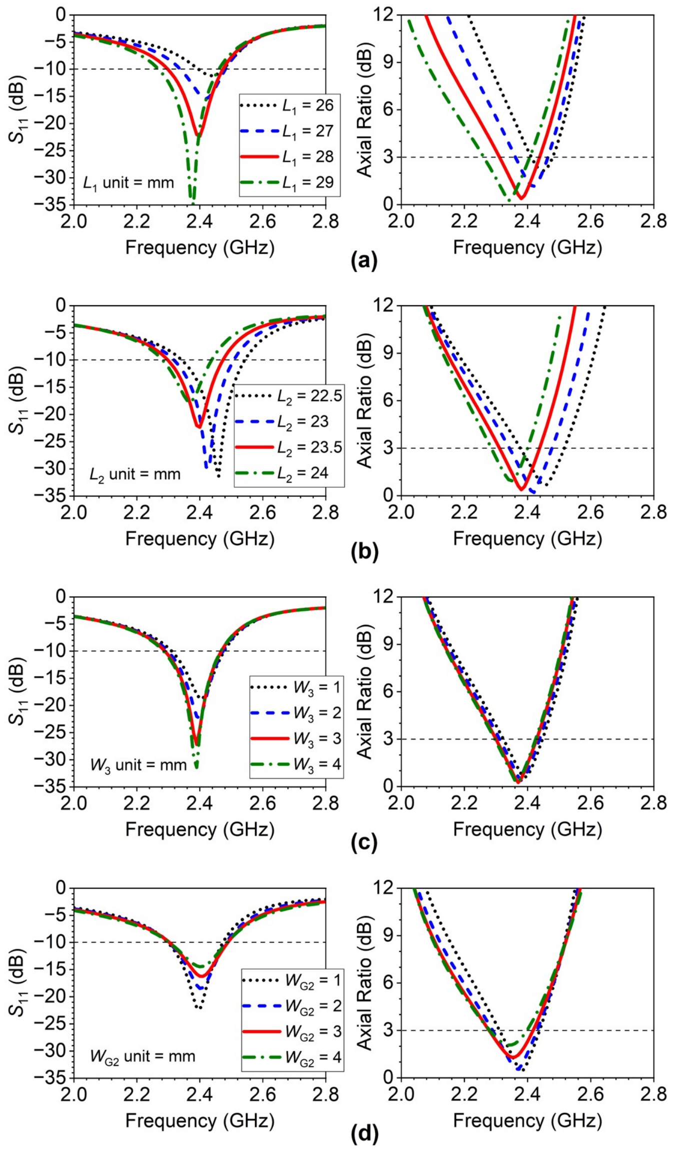

Fig. 4. Simulated S_{11} and axial ratio (AR) responses for (a) varying L_1, (b) varying L_2, (c) varying W_3, and (d) varying W_{G2}.

varying the parameter L_1, which determines the total length of Arm 1 were first studied and the resulting response is shown in Fig. 4(a). As anticipated, a decrease in the resonant frequency and the minimum point of the AR response was observed with an increase in the length of Arm 1 from 26 mm to 29 mm. Varying the parameter L_1 also alters the separation S between the Arm 1 monopole and the ground line of width W_{G2}. It was observed that the separation S has a significant effect on the impedance bandwidth (IBW), $|S_{11}|$, and AR response. As the value of parameter L_1 is increased, the IBW, $|S_{11}|$, AR value, as well as AR bandwidth are improved.

Secondly, the effects of parameter L_2 which determines the total length of Arm 2 were analysed and the corresponding response is shown in Fig. 4(b). Similar to L_1, an increase in the total length of L_2 from 22.5 mm to 24 mm results in a decrease in both the resonant frequency and the AR minimum point along the frequency axis. Thirdly, the effects of varying the parameter W_3, which defines the total width of Arm 3 were studied, and the resulting response is shown in Fig. 4(c). As previously described, Arm 3 was introduced to improve the impedance matching of the antenna, and variations in W_3 primarily controls impedance matching while having minimal impact on the resonant frequency and AR response.

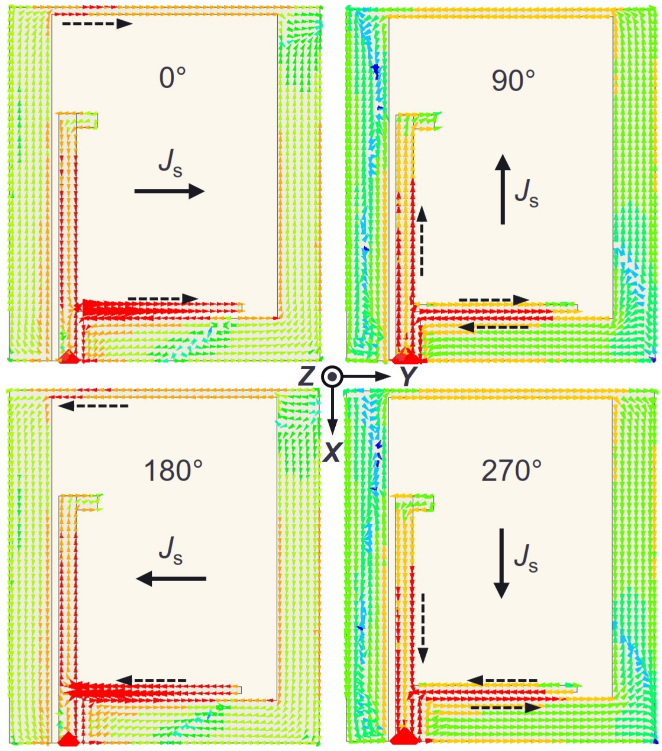

Fig. 5. Simulated surface current density distributions of the proposed antenna at 2.4 GHz at four different phases: 0°, 90°, 180°, and 270°.

Finally, the effects of varying the value of width W_{G2} were analyzed, and the corresponding response is shown in Fig. 4(d). It was observed that changes in the width of the top ground line, W_{G2}, affect the surface current flowing through this ground line. The variation in width W_{G2} was found to primarily influence the AR value, while having minimal impact on the reflection coefficient $|S_{11}|$ of the antenna.

C. Surface Current Distribution and AR Beamwidth

To explain the CP operation of the antenna, the simulated surface current distributions, observed from the +z-direction at four different phases of the RF input (0°, 90°, 180°, and 270°) at 2.4 GHz are presented in Fig. 5. At 0° phase, the predominant surface current flows in the +y-direction. At 90°, a dominant current flow in the −x-direction is observed. It can be seen that at 180° and 270°, the surface current distributions have the same magnitude, but opposite phase compared to those at 0° and 90°, respectively. Since the surface current vector rotates in a counterclockwise direction, the sense of polarization of the antenna is right-handed circular polarization (RHCP) in the direction of the +z-axis.

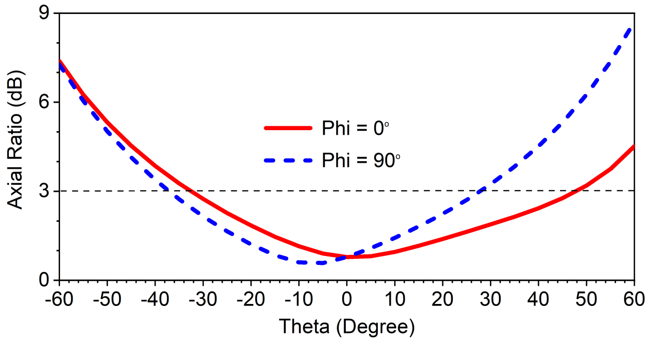

Fig. 6. Simulated ARBW patten of the antenna in the xz-plane ($\phi = 0°$) and yz-plane ($\phi = 90°$).

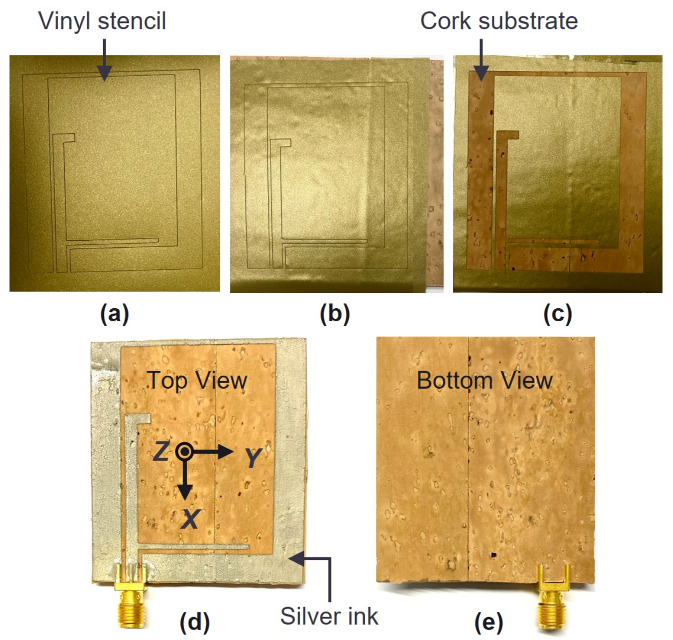

Fig. 7. Antenna fabrication steps: (a) A vinyl stencil with the antenna pattern, (b) stencil attached to a cork substrate, (c) exposed cork areas for silver ink deposition, (d) top view of the antenna prototype, and (e) bottom view of the antenna prototype.

The simulated axial ratio beamwidth (ARBW) of the proposed antenna at 2.4 GHz in the xz-plane ($\phi = 0°$) and yz-plane ($\phi = 90°$) is depicted in Fig. 6. In the xz-plane, the antenna exhibits a 3-dB ARBW of approximately 76° ($\theta = -30°$ to $+46°$). On the other hand, the antenna achieves a 3-dB ARBW of 64° ($\theta = -39°$ to $+25°$) in the yz-plane.

IV. Antenna Fabrication

The antenna was manually screen-printed onto a sustainable cork substrate using a stencil-based technique in a controlled laboratory environment. The fabrication steps of the antenna are illustrated in Fig. 7(a-e). A vinyl stencil, with the desired antenna pattern was created using a Cricut machine [16]. The stencil was then transferred onto the cork substrate using transfer tape. The vinyl was then removed from the areas designated for the application of conductive silver nanoparticles (WIK21285-89A from Henkel [14]). The silver nanoparticles were evenly spread over the exposed cork surface using a squeegee. Subsequently, the fabricated sample was cured in an oven at a temperature of 100°C for 15 minutes to achieve the desired conductivity and ensure proper adhesion of the nanoparticles. Finally, an SMA connector was attached to the antenna using conductive silver epoxy adhesive to facilitate antenna measurements [17]. Then, the fabricated sample was cured in an oven at 80°C for 10 minutes to maximize conductivity and adhesion. The top and bottom views of the final fabricated antenna prototype are shown in Fig. 7(d-e).

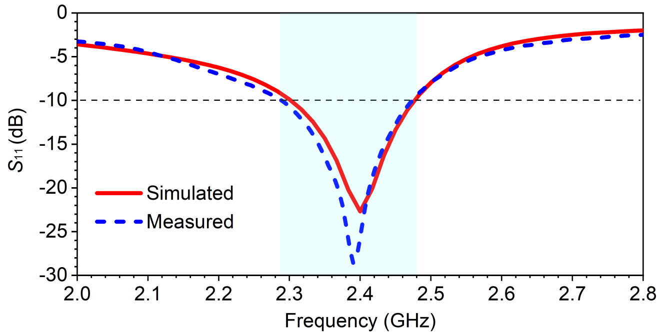

Fig. 8. Simulated versus measured S_{11} response of the antenna.

V. Antenna Measurements

The S_{11} response of the antenna under test (AUT) was measured using a Rohde & Schwarz ZNB8 vector network analyzer (VNA). The simulated and measured S_{11} responses of the antenna are shown in Fig. 8. Close agreement is demonstrated between the simulated and measured S_{11} responses. The measured -10 dB impedance bandwidth is 183 MHz which corresponds to a fractional bandwidth (FBW) of 7.6% at 2.4 GHz. Furthermore, the radiation characteristics of the AUT were measured using an AMS-8050 antenna measurement system. Fig. 9 shows the measurement setup of the AUT inside the anechoic chamber. The 3D rotation of the AUT was controlled using a multi-axis antenna positioner. The antenna is fed through an unbalanced 50-Ω coaxial cable, and to minimize the influence of ground feed cable currents, multiple ferrite beads were included in the setup to suppress shield currents on the feed cable. Fig. 10 presents the simulated and measured RHCP and LHCP radiation patterns of the antenna at 2.4 GHz in the yz and xz-planes. The proposed antenna

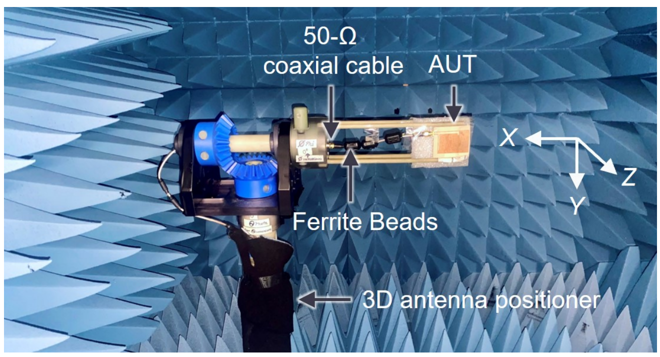

Fig. 9. Antenna under test (AUT) measurement setup in an anechoic chamber.

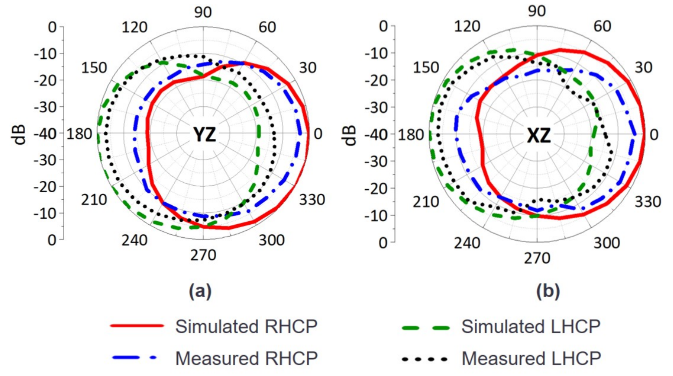

Fig. 10. Simulated and measured RHCP and LHCP radiation patterns of the antenna at 2.4 GHz: (a) yz-plane, and (b) xz-plane.

radiates bi-directionally, producing an RHCP wave in the $+Z$ direction and an LHCP wave in the $-Z$ direction, similar to the CP antennas discussed in [18].

Furthermore, the fabricated antenna exhibited a measured peak realized gain of -1.8 dBi at 2.4 GHz, compared to 0.4 dBi in the simulation. The discrepancy between the simulated and measured radiation patterns, as well as the peak realized gain is thought to be attributed to small manufacturing variations as well as the decreased conductivity of the silver ink due to the curing process which is currently being optimized. The aforementioned factors were not considered but are the subject of future work.

VI. Conclusions

This paper has presented a coplanar waveguide (CPW)-fed circularly polarized (CP) monopole antenna, which was screen-printed on a sustainable cork substrate using silver nanoparticles as the conductive material. Circular polarization was achieved by exciting two orthogonal monopole-type radiating elements. At 2.4 GHz, the developed antenna demonstrated a measured -10 dB fractional impedance bandwidth of 7.6%, a peak realized gain of -1.8 dBi, and a radiation efficiency of 58%. Additionally, this antenna has a 3-dB axial ratio fractional bandwidth of 5.3% at 2.4 GHz. The proposed antenna is suitable for facilitating next-generation wireless communication through integration into sustainable smart flooring systems and wooden structures.

Acknowledgment

This publication has emanated from research conducted with the financial support of Taighde ´ Eireann – Research Ireland and the Department of Agriculture, Food and Marine as well as Enterprise Ireland on behalf of the Government of Ireland under Grant Numbers: SFI 16/RC/3835-2 the SFI Centre VistaMilk; 13/RC/2077 the CONNECT Centre for Future Networks and Communications; SFI/12/RC/2289-2 the Insight Centre for Data Analytics; Grant 16/RC/3918-CONFIRM, and HOLISTICS - Grant EIDT20180291-A. Aspects of this work have also been funded by the EU funded 'Aurora Project' HORIZON-CL2-2022-HERITAGE-01 – 101094245, and the European Union Horizon Europe 'GreenArt project' (101060941). All work is co-funded under the European Regional Development Fund. For the purpose of Open Access, the author has applied a CC BY public copyright licence to any Author Accepted Manuscript version arising from this submission.

References

[1] R. Gonçalves, S. Rima, R. Magueta, P. Pinho, A. Collado, A. Georgiadis, J. Hester, N. B. Carvalho, and M. M. Tentzeris, "RFID-based wireless passive sensors utilizing cork materials," *IEEE Sensors Journal*, vol. 15, no. 12, pp. 7242–7251, 2015.

[2] H. F. Khalili, S. Lemey, O. Caytan, T. Deckmyn, S. Agneessens, D. V. Ginste, and H. Rogier, "Biodegradable dual semicircular patch antenna tile for smart floors," *IEEE Antennas and Wireless Propagation Letters*, vol. 18, no. 2, pp. 368–372, 2019.

[3] B. Mohamadzade, R. M. Hashmi, R. B. Simorangkir, R. Gharaei, S. Ur Rehman, and Q. H. Abbasi, "Recent advances in fabrication methods for flexible antennas in wearable devices: State of the art," *Sensors*, vol. 19, no. 10, p. 2312, 2019.

[4] G. Moloudian, M. Hosseinifard, S. Kumar, R. B. V. B. Simorangkir, J. L. Buckley, C. Song, G. Fantoni, and B. O'Flynn, "Rf energy harvesting techniques for battery-less wireless sensing, industry 4.0, and internet of things: A review," *IEEE Sensors Journal*, vol. 24, no. 5, pp. 5732–5745, 2024.

[5] W. Zhai, Y. Zhong, M. Xu, X. Wei, L. Cai, and C. Xia, "Transforming wastes into functional materials: natural cork-based physical structural components and polymers," *Green Chemistry*, 2024.

[6] O. Caytan, S. Lemey, S. Agneessens, D. Vande Ginste, P. Demeester, C. Loss, R. Salvado, and H. Rogier, "Half-mode substrate-integrated-waveguide cavity-backed slot antenna on cork substrate," *IEEE Antennas and Wireless Propagation Letters*, vol. 15, pp. 162–165, 2016.

[7] S. Lemey, O. Caytan, D. V. Ginste, P. Demeester, H. Rogier, and M. Bozzi, "SIW cavity-backed slot multi-antenna systems for the next generation iot applications," in *2016 IEEE Topical Conference on Wireless Sensors and Sensor Networks (WiSNet)*, 2016, pp. 75–77.

[8] O. Caytan, S. Agneessens, S. Lemey, D. Vande Ginste, P. Demeester, and H. Rogier, "Ultra-wideband cork substrate-integrated-waveguide cavity-backed slot antenna," in *2015 International Conference on Electromagnetics in Advanced Applications (ICEAA)*, 2015, pp. 1104–1107.

[9] S. Rima, A. Georgiadis, A. Collado, R. Goncalves, and N. Carvalho, "Passive UHF RFID enabled temperature sensor tag on cork substrate," in *2014 IEEE RFID Technology and Applications Conference (RFID-TA)*, 2014, pp. 82–85.

[10] L. Lu, Y.-C. Jiao, W. Liang, and H. Zhang, "A novel low-profile dual circularly polarized dielectric resonator antenna," *IEEE Transactions on Antennas and Propagation*, vol. 64, no. 9, pp. 4078–4083, 2016.

[11] D. R. Gawade, B. V. B. Roy Simorangkir, S. Kumar, M. Pigeon, M. Belcastro, N. Rather, J. L. Buckley, and B. O'Flynn, "A battery-less nfc sensor transponder for cattle health monitoring," in *2023 IEEE Applied Sensing Conference (APSCON)*, 2023, pp. 1–3.

[12] R. B. V. B. Simorangkir, D. R. Gawade, S. Kumar, B. O'Flynn, J. L. Buckley, T. Hannon, P. Donovan, and R. Newberry, "Screen printed epidermal antenna for IoT health monitoring," in *2021 IEEE Asia-Pacific Microwave Conference (APMC)*, 2021, pp. 395–397.

[13] *Speag dielectric assessment kit: DAK3.5-TL*, (accessed September 9, 2024). [Online]. Available: https://speag.swiss/products/dak/dak-tl-2/.

[14] *Conductive Silver Nanoparticle Ink*, (accessed September 9, 2024). [Online]. Available: https://www.henkel-adhesives.com/uk/en.html.

[15] *ANSYS HFSS*, (accessed September 9, 2024). [Online]. Available: http://www.ansys.com/products/electronics/ansys-hfss.

[16] *Cricut Maker*, (accessed September 9, 2024). [Online]. Available: https://cricut.com/en-ie/cutting-machines/cricut-maker/cricut-maker-3.

[17] *Conductive Epoxy: CW2400*, (accessed September 9, 2024). [Online]. Available: https://www.chemtronics.com/circuitworks-conductive-epoxy-2.

[18] M. Nosrati and N. Tavassolian, "Miniaturized circularly polarized square slot antenna with enhanced axial-ratio bandwidth using an antipodal y-strip," *IEEE Antennas and Wireless Propagation Letters*, vol. 16, pp. 817–820, 2017.